Suzana Jakovljević ✉
Dražen Mezdić
Gorana Baršić
Hrvoje Skenderović

https://doi.org/10.21278/TOF.454031721
ISSN 1333-1124
eISSN 1849-1391

INVESTIGATION INTO THE EFFECTS OF LASER TEXTURING ON THE WETTABILITY OF TI-6AL-4V ALLOY

Summary

Laser surface texturing is a technology that enables us to achieve very complex surface geometries. In this study, geometries created on the Ti-6Al-4V surface were in the form of parallel grooves. Those geometries were obtained by changing the laser beam speed and the number of passes (one or two). The effects of laser texturing on the roughness and the contact angle of Ti-6Al-4V surfaces on the first day and after 80 days were investigated. The results of this study indicate that the samples treated with two passes of the laser beam and at a lower speed scan show regularities of roughness profile geometry while other laser-treated samples do not. It is shown that the surfaces laser-textured with either one or two passes of the laser beam show no significant changes in the surface wettability after 80 days. The statistical test proves that there is a significant difference (level $\alpha = 0.05$) between the contact angles on the untreated sample on the first day and after 80 days of treatment.

Key words: *Ti-6Al-4V, laser surface texturing, surface topography, roughness, wettability*

1. Introduction

All components used in transportation, production, and energy generation are made up of moving parts whose surfaces are in contact with each other. To extend their service life, it is necessary to study the friction between the materials in contact. Friction and wear depend on the topography of surfaces and on a given tribo-pair. Rough surfaces in contact cause increased wear of the material, and it is well known that surfaces are not ideally smooth. From the microscopic point of view, rough surfaces are described by a series of irregularities of different shapes, arrangements, and sizes [1]. Therefore, tribology is increasingly focused on the study of surfaces and on surface preparation. In the field of surface preparation, the use of conventional procedures is well documented in the literature, while the use of advanced technologies and its effect on the behaviour of treated surfaces are less commonly known [2]. In the surface treatment of titanium and its alloys, it is mechanical pre-treatment that is predominantly applied. Titanium alloys are widely used in medical applications as implants because of their good mechanical properties such as strength and their biocompatibility. However, a problem with these alloys is their low wear resistance; in order

to improve it, the roughness of surfaces in contact should be reduced by pre-treatment [3]. Micro-hardness, roughness, and contact angle tests carried out on the pre-treated surfaces show that their negative tribological properties have been improved [4]. The low wear resistance of Ti6Al4V alloy has limited the use of this material in medicine. In the human system, when Ti6Al4V is worn, corrosion can occur, which can lead to an accelerated implant breakdown [5]. To improve the topography and surface roughness of Ti6Al4V alloy, new technologies, such as laser processing, are increasingly being used [6]. Laser processing techniques allow a contactless treatment of the surface of the material. This technology is a clean and precise procedure due to the excellent control of heat absorption in the heat-affected zone and the ability to focus the laser beam on small surfaces [7]. Laser processing can be used to control surface roughness by texturing different shapes in different dimensions [8]. Microstructures resulting from laser texturing can act as reservoirs for wear particles of the materials in contact [9]. Laser surface treatment with a pulse duration ranging from a few microseconds to a few nanoseconds can form coarse layers, such as ring edges around holes or micro-dots, which increase the coefficient of friction of metals [10]. Laser-induced phase transitions, such as melting followed by rapid solidification, can modify the structure of the material [11]. Such an effect leads to an increase in surface hardness and improved wear resistance [12]. The structures produced by laser can affect the surface contact angle, i.e. the surface wettability, which can be relevant for the use of lubricants [13]. Chemical reactions after laser treatment can have an additional effect on the wettability of the surface. Laser-treated surface layers can show a wide range of mechanical properties and act as grooves for the accumulation of harmful substances contained in some lubricants [14]. The results presented in [15] showed that the laser treatment in the micro- and nano-areas resulted in high, but uniform, surface roughness. However, laser-treated metal surfaces still exhibit higher wear than the desired. As a result, various coatings, such as diamond-like carbon, titanium nitride, and titanium carbo-nitride coatings, have recently been applied to titanium alloys as well as lubricants. These coatings have excellent properties of reducing surface friction and allow the application of titanium and its alloys in industries where tribological issues are of major importance [16]. However, the roughness of a surface has a significant influence on its adhesive properties and on the thickness of the coating itself. As a result, an increasing number of studies are focused on the use of an ultra-short laser beam, which produces extremely low roughness when applied to metals [17]. Femtosecond (fs) lasers have an ultra-short pulse duration and for that reason they may be the tool for processing almost any material [18]. A remarkable feature of femtosecond lasers is that they have a minimal heat-affected zone. In addition, femtosecond lasers have a higher degree of precision in the texturing and modification of the treated material. The heat-affected zone is much smaller than that created by irradiation with nanosecond-to-microsecond laser pulses [19]. With femtosecond lasers it is possible to produce the shapes of random grooves, waves, and parallel grooves on a metal surface. Geometries obtained by changing the parameters of power, speed, and size of the laser beam bring about the effect of a uniform surface with very low roughness; depending on the desired outcome, hydrophobic or hydrophilic surfaces can be created [20]. Moreover, the shapes created on the surface increase adhesion of the coating to titanium alloys without changing the microstructure of titanium substrate [21]. The result is an excellent wettability of the coating surface, and therefore its adhesion, which gives the Ti-6Al-4V alloy high wear resistance [22].

The present research is aimed to investigate the laser surface texturing of the Ti-6Al-4V alloy and its effect on the topography and wetting properties of the resulting surface after 80 days.

2. Materials and methods

In the present investigation, the Ti-6Al-4V alloy was chosen as the experimental material; samples were produced in dimensions 17 x 17 x 7 mm. Prior to laser treatment, the Ti-6Al-4V samples were abraded with silicon carbide sandpapers of various grits on a Buehler Phoenix Alpha machine. The process parameters were as follows: a rotating speed of 300 rpm and the P320, P1000, P2000, and P4000 grit sandpaper. After grinding, the samples were mechanically polished on a Struers DAP-V machine in two phases. During the first phase, polishing was performed using an MD-Largo plate and 9 μm diamond paste. In the second phase, polishing was performed using an MD-Chem plate and liquid silica with a particle granulation of 0.03 μm. In both phases of the mechanical polishing process, the speed was 150 rpm and the pressure force was 20 N. The samples were ultrasonically cleaned in an ethylene bath and air-dried before laser treatment.

A Ti:Sapphire laser system (SpectraPhysics Spitfire seeded by Tsunami) operating at a 1kHz pulse repetition rate was used in the experiments. The laser system delivered 120fs pulses at 800 nm with a maximum laser energy per pulse of 0.8 mJ. The energy stability was within 2%. In typical measurements, much less energy was needed and the original beam was attenuated by a set of absorptive neutral density filters. The laser pulses were focused on the sample surfaces by passing them through a 500 mm focal length lens to a focal spot of 80μm in diameter. The texturing was performed line by line, and the distance between lines was h = 15 μm. The spot size of the beam in the focal area was 80 μm in diameter; thus, for a power of 16 mW, the fluence is equal to 0.28 J/cm^2. The distance between two consecutive spot centers d is defined as $d = v/f$, where v is the scan velocity, and f is the repetition rate of the laser; hence, d equals 5 and 10 μm for velocities of 5 and 10 mm/s, respectively. The effective number of pulses per unit area is defined as:

$$N_{eff} = \frac{\pi \times \omega_o^2}{d \times h} \tag{1}$$

where ω_0 is the radius of the focal spot. This means that every point on the surface is exposed to a certain effective number of pulses. The effective number of pulses (N_{eff}) at a velocity of 5 mm/s was 75.5, and at 10 mm/s it was 37.7. The laser parameters, i.e. the laser irradiation power and scanning speed, together with the number of passes were varied to create lines on the surface. Samples without surface texturing were used as references.

The tested samples are:

- RS – Mechanically pre-treated samples.
- LST 16-5-1 - Laser power, P=16 mW; scanning speed, v=5 mm/s; no. of passes: 1;
- LST 16-5-2 - Laser power, P=16 mW; scanning speed, v=5 mm/s; no. of passes: 2;
- LST 16-10-1 - Laser power, P=16 mW; scanning speed, v=10 mm/s; no. of passes: 1;
- LST 16-10-2 - Laser power, P=16 mW; scanning speed, v=10 mm/s; no. of passes: 2;

A schematic picture of the surfaces obtained after the laser treatments with one and two passes is shown in Figure 1.

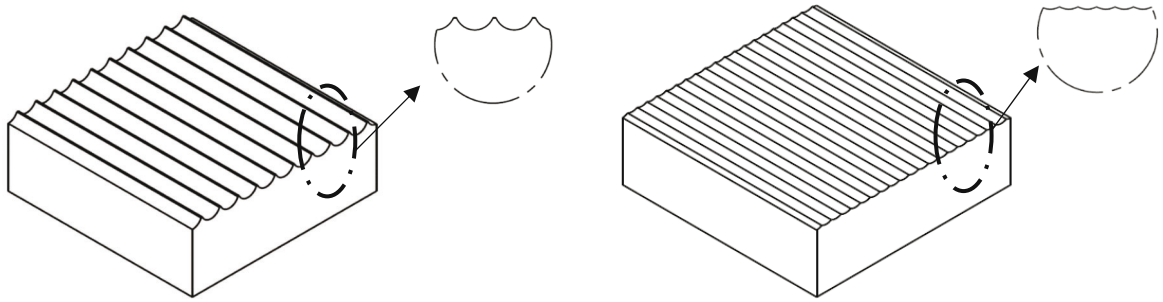

a) b)

Fig. 1 3D representations and details of samples laser-treated with: a) one-pass and b) two-passes

After laser treatment, the topography of surface was determined using a TESCAN VEGA 5136 MM scanning electron microscopy system.

Surface roughness measurements were performed using a stylus instrument, Mahr Perthen Perthometer S8P. A Gaussian filter was used with a cut-off value, λ_c, of 0.25 mm, evaluation length, l_n, of 1.25 mm, and a tip radius, r, of 5 μm. Samples were measured before and after laser treatment. For each sample, six measurements uniformly distributed over the sample surface were scanned. The arithmetical mean and standard deviation of roughness parameters R_a, R_z, and R_p were calculated.

The Vickers method was used to measure microhardness on a hardness tester manufactured by Indentec, type ZHVμ-ST, serial number 206030, according to the EN ISO 6507-1 standard. The compressive force of the indenter was 10 kg (HV1) and the dwell time was 15 seconds. Lengths of the impression diagonals and the hardness of samples were determined using a measuring microscope. Measurements were performed on a reference sample and on the samples treated with the laser beam. Each sample was measured 5 times; based on the measurement results, average values of hardness were obtained.

X-ray diffraction analysis (XRD) was carried out on a Shimadzu XRD 6000 diffractometer with CuKα radiation, operating at 40 kV and 30 mA; the aim of XRD was to identify the phases of the Ti6Al4V alloy before and after laser processing. Data were collected in a step-scan mode between 20 and 100 °2θ with steps of 0.02 °2θ and a counting time of 0.6 s.

The contact angle between the liquid and the Ti-6Al-4V surface was measured using a Dataphysics OCA goniometer. Measurements were performed as follows: distilled water was used as the test liquid, the drop volume was 2 μl, and the time to establish balance was 10-30 seconds. During the measurements, the samples and the droplet were visually monitored via an optical system (which allows a magnification of 0.7 - 4.5x) connected to a computer. The results indicate the mean value of the contact angle obtained in 7 measurements. The tests were carried out at an ambient laboratory temperature, T, of 21ºC and at a relative humidity, rH, of 45%. The equilibrium contact angles were measured after 20 s from water drop depositions. The measurements of contact angle were repeated after 80 days in the same conditions.

In order to determine the differences between the contact angles of various textured and non-textured surfaces on the first day and after 80 days, the mean differences between two sets of observations were compared. A statistical test comparing the means of two dependent samples was used to determine whether or not there are significant differences between the true means of the paired samples which were observed.

In a paired sample t-test, each subject or entity is measured twice, resulting in pairs of observations. The paired sample t-test has two competing hypotheses, the null hypothesis and the alternative hypothesis. The null hypothesis assumes that the true mean difference between the paired samples is zero. In this model, all observable differences are explained by random

variation. Conversely, the alternative hypothesis assumes that the true mean difference between the paired samples is not equal to zero. The alternative hypothesis can take one of several possible forms depending on the expected outcome. If the direction of the difference does not matter, a two-tailed hypothesis is used. The upper-tailed or the lower-tailed hypothesis can be used to increase the power of the test. The null hypothesis remains the same for each type of alternative hypothesis. The p-value gives the probability of observing the test results under the null hypothesis. A low p-value indicates decreased support for the null hypothesis. However, the possibility that the null hypothesis is true and that we have simply obtained a very rare result can never be ruled out completely. The cut-off value for determining statistical significance is usually decided upon and a value of 0.05 (or less) is chosen. This corresponds to a 5% (or less) chance of obtaining a result like the one that was observed in the case when the null hypothesis was true.

3. Results and discussion

3.1 Surface characterisation

In this study, the SEM analysis of all tested samples was carried out. The SEM analysis results of the laser-treated sample are shown in Figure 2.

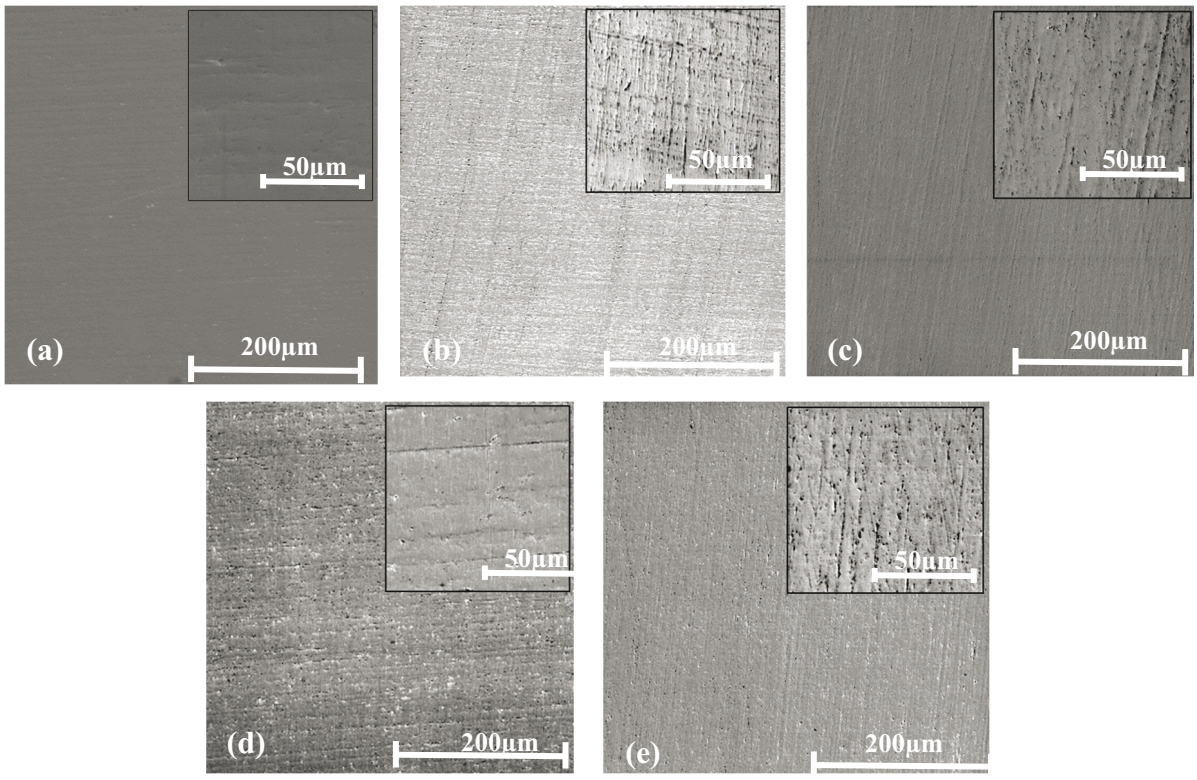

Fig. 2 Top-view SEM images of the Ti6Al4V alloy surface after femtosecond laser texturing: (a) Reference sample (RS), (b) LST-16-5-1, (c) LST-16-5-2, (d) LST-16-10-1, (e) LST-16-10-2.

Under the laser irradiation at a power, P, of 16 mW and a variable scan speed, the surface of the Ti6Al4V samples exhibited linear grooved nanostructures. There are visible changes on the surfaces of all laser-treated samples (LST-16-5-1, LST-16-5-2, LST-16-10-1, and LST-16-10-2) with respect to the reference sample (RS). There are no clearly visible traces of lines as in [19] due to the low power of the laser beam used for the treatment of the sample surfaces. Lines and pores observed on all tested samples (Figure 2) could originate from mechanical pre-treatment, or they could be attributed to microstructural inhomogeneity. Table 1 shows the results of the surface roughness measurements after laser surface treatment expressed by the parameters R_a, R_z, and R_p.

Table 1 Parameters of roughness after laser surface treatment of the Ti6Al4V samples

	Roughness		
	R_a (µm)	R_z (µm)	R_p (µm)
RS	0.026 ± 0.002	0.198 ± 0.012	0.083 ± 0.009
LST 16-5-1	0.034 ± 0.002	0.289 ± 0.016	0.132 ± 0.073
LST 16-5-2	0.036 ± 0.001	0.249 ± 0.024	0.167 ± 0.065
LST 16-10-1	0.022 ± 0.002	0.176 ± 0.017	0.068 ± 0.009
LST 16-10-2	0.040 ± 0.002	0.277 ± 0.016	0.133 ± 0.019

All values are denoted as mean ± SD for $n = 6$.

Values of measurements taken after six repetitions on different positions on the sample surface in the direction perpendicular to the surface texture are shown in Table 1. One can see that the mean roughness profile R_a varies from 0.022 µm to a maximum roughness of 0.040 µm. The surface of the LST-16-5-1 sample treated with one pass of laser beam, and those of the LST-16-5-2 and LST-16-10-2 samples treated with two passes have higher values of roughness parameters R_a, R_z, and R_p than the reference sample (RS). The roughness parameters of the sample LST-16-10-1 show no significant changes in their values compared to the reference sample (RS). The low energy laser beam applied to the surface of the LST-16-10-1 sample has not significantly affected the sample surface [22]. Significant differences between the reference sample (RS) and the samples treated with laser in one pass (LST 16-5-1) and two passes (LST 16-5-2, LST 16-10-2) can be noticed in the roughness profiles shown in Figure 3 below.

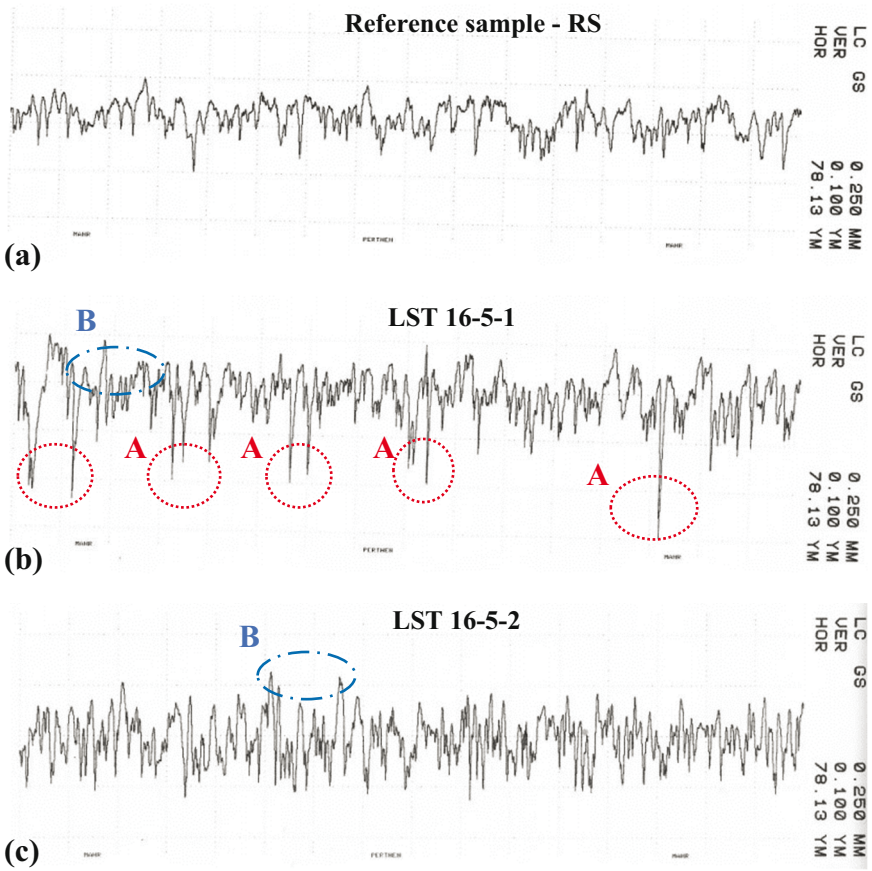

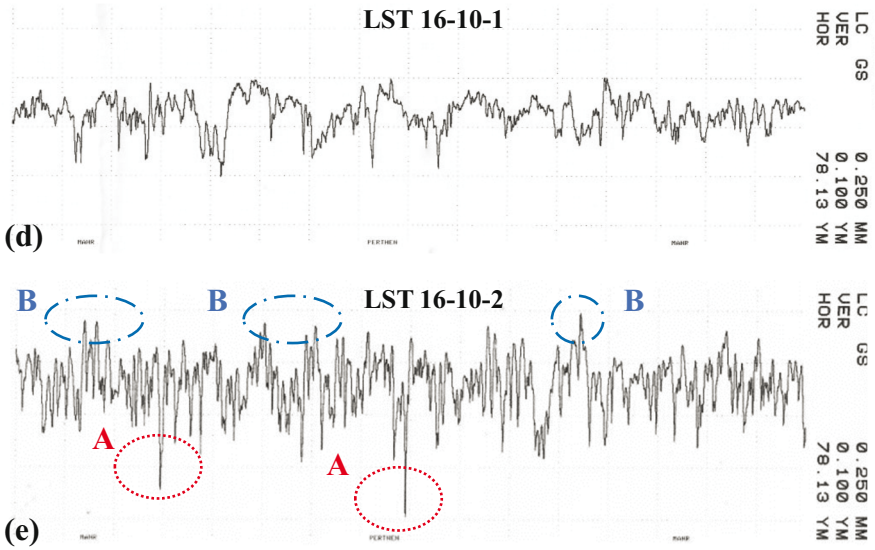

Fig. 3 Surface topography of the Ti6Al4V alloy samples after laser surface treatment: (a) Reference sample RS, (b) LST 16-5-1, (c) LST 16-5-2, (d) LST 16-10-1, (e) LST 16-10-2.

Figure 3 shows the changes in the roughness profile after laser surface treatment in relation to the reference sample (RS). Deep grooves on the roughness profile of the laser-treated samples LST 16-5-1 and LST-16-10- are marked with A in Figures 3(b) and 3(e). The mark A indicates potential pores in the material itself or a stronger effect of the laser beam intensity on the phases and microstructure of the Ti6Al4V alloy. High peaks (marked with B) of irregularities are shown in Figures 3(b), 3(c) and 3(e); these peaks could be the effect of droplets formed by the melting of the material after linear grooves have been produced by laser processing [20]. Laser irradiation at a high power intensity and lower scan speeds of 5 mm/sec and 10 mm/sec increases the interaction time between the surface and the laser beam. A longer interaction time and a higher laser intensity result in higher dissolution and improper re-solidification [23]. In addition to the interaction time and laser intensity, other laser irradiation parameters such as power, scanning speed, number of passes, and procedure of laser passages also have an important role in laser texturing. The roughness profile of the sample LST 16-5-2 shown in Figure 3(c) has almost a regular profile of grooves and peaks, which is not the case with the samples LST 16-5-1 and LST 16-10-2 (Figure 3(b) and 3(e)). Comparing the roughness profile of the reference sample (RS) in Figure 3(a) with those of the samples in Figure 3(c) and 3(d), one can note the regularity of profile geometry of the samples LST 16-5-2 and LST 16-10-1 (Figures 3(c), and 3(d)) while irregularities can be noted on the sample LST-16-10 -2 shown in Figure 3(e). In addition to the similarity in the geometry of roughness profile, the measurements of the LST 16-10-1 sample shown in Table 1 show similarity with the reference sample (RS). It can be assumed that the one-pass laser beam at a power of 16 mW and a scanning speed of 10 mm/s has no significant effect on the roughness profile.

3.2 XRD analysis

The X-ray diffraction confirmed the presence of α-Ti and β-Ti phases in the Ti6Al4V alloy. The α phase of Ti had a hexagonal close-packed crystal cell, where a =b= 0.29505 nm and c = 0.46826 nm, according to the reference code JCPDS #44-1294. The XRD measurements also confirmed the β phase structure with a body-centred cubic crystal cell, where a = 0.33065 nm according to the reference code JCPDS #44-1288. Figure 4 shows the phases of Ti6Al4V alloy observed on the reference and laser-treated samples.

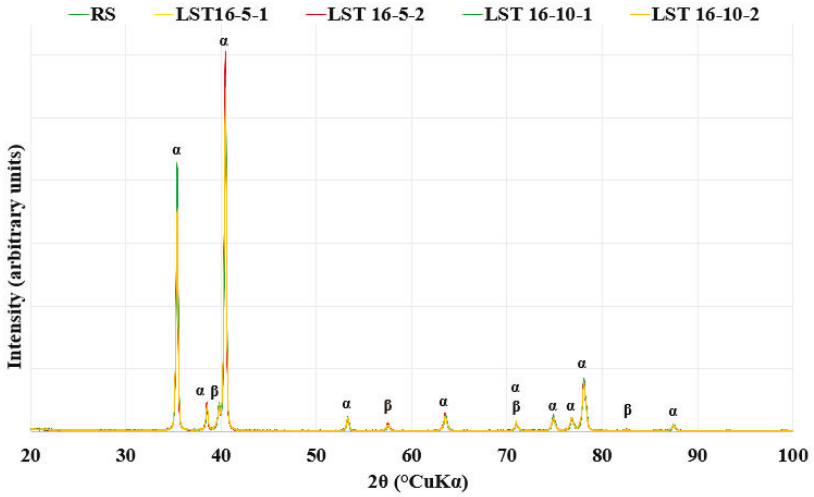

Fig. 4 X-ray diffraction analysis of phases on the reference and laser-treated Ti6Al4V samples

The X-ray diffraction shows that the reference sample and the samples treated with the laser beam have the same phases of microstructure. Based on that, one can conclude that the defined parameters used for laser processing do not affect the microstructure of the material.

3.3 Vickers hardness test

The values of Vickers hardness measured after six repetitions at different positions on the reference sample surface and the laser-treated surfaces are shown in Table 2. No significant changes in HV1 were observed on the laser-treated surfaces relative to the reference sample. The hardness values of all samples are around 300 HV1. The effect of surface hardening at low intensity of laser beam was not confirmed, and, consequently, the formation of α martensitic phase was not noted (Figure 4); the same findings were reported in [24]. According to XRD analyses, the phases of microstructure of the tested samples are not changed. There are no traces of cracks on the Ti6AL4V samples around the indentations made by the Vickers hardness tests.

Table 2 Vickers hardness HV1 of reference and laser-treated Ti6Al4V surfaces

	Microhardness HV1
RS	295 ± 4.33
LST 16-5-1	300 ± 2.91
LST 16-5-2	299 ± 5.66
LST 16-10-1	300 ± 3.14
LST 16-10-2	301 ± 2.47

3.4 Contact angle of laser-treated Ti6Al4V surfaces

The contact angle measurements of four laser-treated samples were performed to determine the wettability of the surface. It was observed that the wetting behaviour of laser-treated Ti6Al4V surfaces had changed over time; this was confirmed by the analyses performed on the first day of treatment and after 80 days. After 80 days, the contact angles of the laser-treated surfaces had changed from low contact angles to high contact angles; this happened due to the formation of oxide layers resulting from the interaction of molecules available in the ambient environment [23]. The values of contact angles were measured using distilled water on the surface of five samples after 80 days to determine the effect of time on the formation of oxide layers. The graph in Figure 5 shows the contact angle data of various laser-treated surfaces (LST-16-5-1, LST-16-5-2, LST-16-10-1, and LST-16-10-2) and the reference surface (RS).

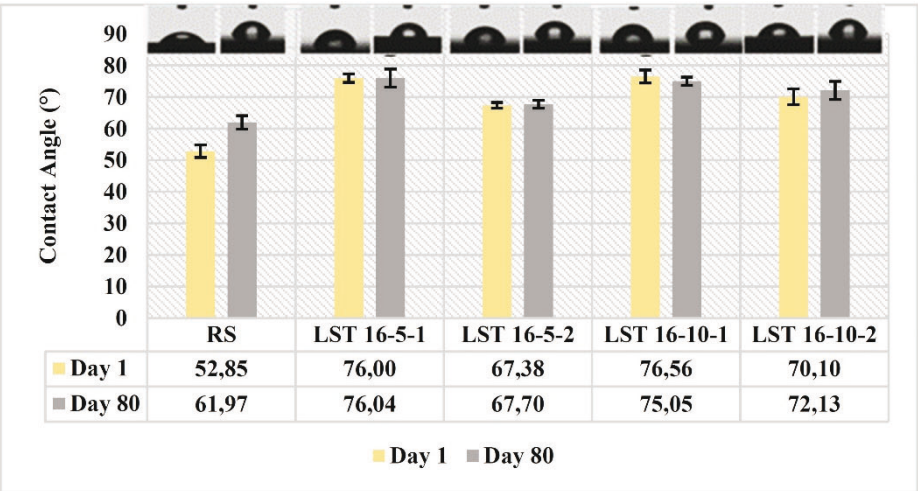

Fig. 5 Comparison of contact angles of various laser-treated samples and the reference sample on the first day and after 80 days

In Figure 5 one can see that all tested samples have hydrophilic surfaces, i.e. wettable surfaces. The contact angles of samples treated with one pass of laser beam, LST-16-5-1 (CA of 76°) and LST-16-10-1 (CA of 76.56°), show the highest contact angles and the reference sample the lowest. The samples LST-16-5-2 and LST-16-10-2 treated with two passes of laser beam show lower values of contact angle compared to the samples laser-treated with one pass. The surfaces of all samples remain hydrophilic even 80 days after laser treatment. The contact angle on the reference sample (RS) surface shown in Figure 5 had increased by 14.71% after 80 days under ambient conditions. Samples treated with two passes of laser beam show a small increase in the contact angle, LST 16-5-2 an increase of 0.48 % and LST 16-10-2 of 2.82%. There are no visible changes in the contact angle of the sample LST 16-5-1 80 days after laser treatment compared to the first day. A slight decrease in the contact angle of 1.97% can be noted on the sample LST 16-10-1 80 days after laser treatment. The low values of the contact angles 80 days after laser treatment can be explained by the fact that the subsequent exposition to air leads to the formation of TiO_2 and unsaturated chemical compounds on the surface of the alloy; this is associated with the hydrophilic behaviour of the surface, i.e. its wettability [24]. It seems that this mechanism depends on the fluence of a laser pulse, or rather on the irradiated energy which seems to determine the level of oxygen on the surface [25].

After measurements, a statistical comparison of mean contact angles on the first day and after 80 days was carried out using the t-test. Statistical significance of the t-test is determined by analysing the *p*-values. Lower *p*-values, less than $\alpha = 0.05$, at the 5% significance level, lead to the rejection of the null hypothesis. Summary statistics (central tendency measures, scatter measures, shape measures) in Table 3 shows a range of different statistics commonly used to summarize samples of variable data.

Table 3 Summary statistics of contact angles of laser-treated samples and the reference sample on the first day and after 80 days

	Contact Angle (°)									
Sample	**RS**		**LST 16-5-1**		**LST 16-5-2**		**LST 16-10-1**		**LST 16-10-2**	
	Day 1	**Day 80**	**Day 1**	**Day 80**	**Day 1**	**Day 80**	**Day 1**	**Day 80**	**Day 1**	**Day 80**
Number of samples	7		7		7		7		7	
Average	52.85	61.97	76.00	76.04	67.38	67.70	76.56	75.05	70.10	72.13
Median	52.50	62.69	75.89	77.27	67.50	67.75	76.53	74.53	68.82	71.35
Variance	3.91	4.52	1.88	8.39	0.85	1.59	4.27	1.63	6.46	8.15
Standard deviation	1.98	2.13	1.37	2.90	0.92	1.26	2.07	1.28	2.54	2.86

	Contact Angle (°)									
Sample	**RS**		**LST 16-5-1**		**LST 16-5-2**		**LST 16-10-1**		**LST 16-10-2**	
	Day 1	**Day 80**	**Day 1**	**Day 80**	**Day 1**	**Day 80**	**Day 1**	**Day 80**	**Day 1**	**Day 80**
Number of samples	7		7		7		7		7	
Coeff. of variation, %	3.74	3.43	1.80	3.81	1.37	1.86	2.70	1.70	3.63	3.96
Minimum	50.95	58.22	73.80	71.02	65.97	65.28	72.97	73.42	66.95	68.45
Maximum	57.26	65.15	77.85	79.69	68.61	69.35	78.87	77.03	74.16	76.67
Lower quartile	51.60	60.61	75.19	73.94	66.64	67.12	75.31	74.05	68.56	69.94
Upper quartile	53.02	63.24	77.05	78.20	68.14	68.64	78.45	76.13	71.82	74.27
Interquartile range	1.42	2.63	1.87	4.25	1.51	1.52	3.14	2.09	3.26	4.33

To show the important features of numerical data, a box-and-whisker plot is shown in Figure 6. The box-and-whisker plots summarize data samples through 5 data set features: minimum, maximum, median, lower quartile, and upper quartile. The box-and-whisker diagrams visually show the data distribution through their quartiles.

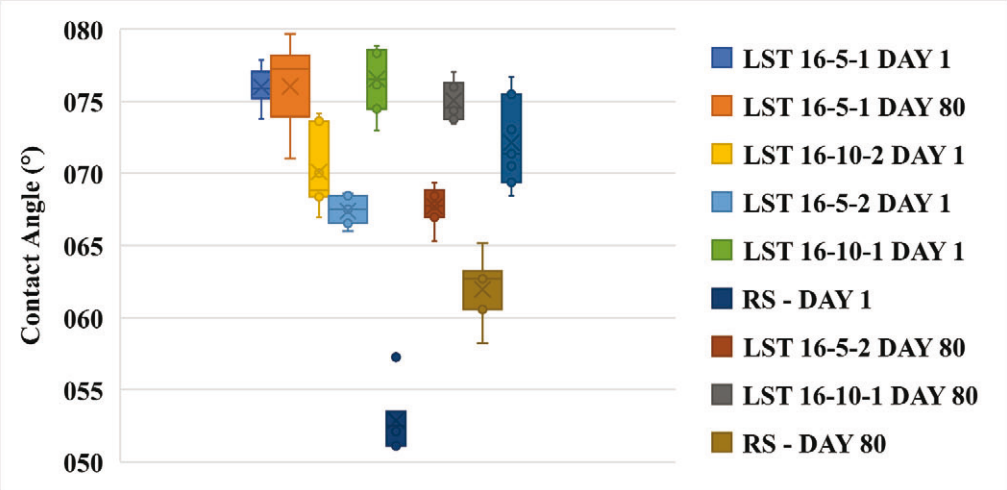

Fig. 6 Box-and-whisker plot of contact angles of various laser-treated samples and the reference sample on the first day and after 80 days

The t-test for testing the null hypothesis was also performed. The hypotheses that were tested are:

- Null hypothesis H0: there is no significant difference between the groups ($p > \alpha = 0.05$)
- Alternative hypothesis H1: there is a significant difference between the groups ($p < \alpha = 0.05$)

Results of the t-paired test for the contact angle performed for testing the null hypothesis on the first day and 80 days after laser treatment are shown in Table 4.

Table 4 T-paired test for the contact angle performed for testing the null hypothesis

	***t* - paired test**				
Sample	**RS**	**LST 16-5-1**	**LST 16-5-2**	**LST 16-10-1**	**LST 16-10-2**
***p* - value**	0.003	0.947	0.235	0.620	0.462
Null hypothesis: H_0	-	Accept H_0	Accept H_0	Accept H_0	Accept H_0
Alternative hypothesis: H_1	Accept H_1	-	-	-	-

It was proved that there was no significant difference between contact angles of various textured surfaces on the first day and after 80 days at the level of significance $\alpha = 0.05$. The p-value of the reference sample (RS) is $p = 0.003$, which is less than 0.05, and thus the hypothesis H0 about the mean equality of the contact angle measured on the first day and after 80 days

was rejected. At the level of statistical significance, it is indicated that there is no significant difference between the mean values of contact angles on the samples LST 16-5-1 (p = 0.947), LST 16-5-2 (p = 0.235), LST 16-10-1 (p = 0.620), and LST 16-10-2 (p = 0.462) and the hypothesis H0 was accepted.

4. Conclusion

The purpose of this research was to investigate the femtosecond-laser texturing of the Ti-6Al-4V alloy and its effect on the topography and wetting properties of the resulting surface. As a result of this study, the main new findings about the nature of laser-treated sample surfaces are:

- SEM images show changes in the surface topography of laser-treated samples.
- The smallest irregularity in the roughness profile geometry is shown on the sample treated with two passes of laser beam at a scanning speed of 5 mm/sec.
- The defined parameters of laser processing do not affect the microstructure phases and hardness of the material.
- The highest value of contact angle on the first day is exhibited by the sample treated with one pass of laser beam.
- Laser-treated samples are hydrophilic on the first day and after 80 days.
- The statistical test showed that a significant difference between contact angles is noted only on the reference sample (RS) on the first day and after 80 days.

Further research is required to fully explain the changes in the microstructure of Ti alloy caused by laser pre-treatment. Future work is planned in order to examine the influence of different values of laser beam power in dependence on low treatment speeds.

REFERENCES

[1] K. Holmberg and A. Erdemir, "Influence of tribology on global energy consumption, costs and emissions," *Friction*, vol. 5, no. 3, pp. 263–284, Sep. 2017, https://doi.org/10.1007/s40544-017-0183-5.

[2] M. Basiaga, W. Walke, Z. Paszenda, and A. Kajzer, "The effect of EO and steam sterilization on the mechanical and electrochemical properties of titanium Grade 4," *Mater. Tehnol.*, vol. 50, no. 1, pp. 153–158, Feb. 2016, https://doi.org/10.17222/mit.2014.241.

[3] Z. M. Jin, J. Zheng, W. Li, and Z. R. Zhou, "Tribology of medical devices," *Biosurface and Biotribology*, vol. 2, no. 4, pp. 173–192, Dec. 2016, https://doi.org/10.1016/j.bsbt.2016.12.001.

[4] J. M. Vazquez-Martinez, J. S. Gomez, P. F. M. Ares, S. R. Fernandez-Vidal, and M. B. Ponce, "Effects of Laser Microtexturing on the Wetting Behavior of Ti6Al4V Alloy," *Coatings*, vol. 8, no. 4, p. 145, Apr. 2018, https://doi.org/10.3390/coatings8040145.

[5] J. Zhou, Y. Sun, S. Huang, J. Sheng, J. Li, and E. Agyenim-Boateng, "Effect of laser peening on friction and wear behavior of medical Ti6Al4V alloy," *Opt. Laser Technol.*, vol. 109, no. December 2017, pp. 263–269, Jan. 2019, https://doi.org/10.1016/j.optlastec.2018.08.005.

[6] C. G. Moura, O. Carvalho, L. M. V. Gonçalves, M. F. Cerqueira, R. Nascimento, and F. Silva, "Laser surface texturing of Ti-6Al-4V by nanosecond laser: Surface characterization, Ti-oxide layer analysis and its electrical insulation performance," *Mater. Sci. Eng. C*, vol. 104, no. June, p. 109901, Nov. 2019, https://doi.org/10.1016/j.msec.2019.109901.

[7] J. Vázquez Martínez, J. Salguero Gómez, M. Batista Ponce, and F. Botana Pedemonte, "Effects of Laser Processing Parameters on Texturized Layer Development and Surface Features of Ti6Al4V Alloy Samples," *Coatings*, vol. 8, no. 1, p. 6, Dec. 2017, https://doi.org/10.3390/coatings8010006.

[8] L. Tiainen *et al.*, "Novel laser surface texturing for improved primary stability of titanium implants," *J. Mech. Behav. Biomed. Mater.*, vol. 98, no. November 2018, pp. 26–39, Oct. 2019, https://doi.org/10.1016/j.jmbbm.2019.04.052.

[9] F. Dai, Z. Zhang, X. Ren, J. Lu, and S. Huang, "Effects of laser shock peening with contacting foil on micro laser texturing surface of Ti6Al4V," *Opt. Lasers Eng.*, vol. 101, no. June 2017, pp. 99–105, Feb. 2018, https://doi.org/10.1016/j.optlaseng.2017.09.024.

[10] A. Temmler, D. M. Liu, S. Drinck, J. B. Luo, and R. Poprawe, "Experimental investigation on a new hybrid laser process for surface structuring by vapor pressure on Ti6Al4V," *J. Mater. Process. Technol.*, vol. 277, p. 116450, 2020, https://doi.org/10.1016/j.jmatprotec.2019.116450.

[11] M. Chérif, C. Loumena, J. Jumel, and R. Kling, "Performance of Laser Surface Preparation of Ti6Al4 V," *Procedia CIRP*, vol. 45, pp. 311–314, 2016, https://doi.org/10.1016/j.procir.2016.02.354.

[12] A. Grabowski, M. Sozańska, M. Adamiak, M. Kępińska, and T. Florian, "Laser surface texturing of Ti6Al4V alloy, stainless steel and aluminium silicon alloy," *Appl. Surf. Sci.*, vol. 461, no. May, pp. 117–123, Dec. 2018, https://doi.org/10.1016/j.apsusc.2018.06.060.

[13] A. S. Goldstein, "Cell Adhesion," in *SpringerReference*, Berlin/Heidelberg: Springer-Verlag, 2016, pp. 503–519.

[14] J. Salguero, I. Del Sol, J. M. Vazquez-Martinez, M. J. Schertzer, and P. Iglesias, "Effect of laser parameters on the tribological behavior of Ti6Al4V titanium microtextures under lubricated conditions," *Wear*, vol. 426–427, no. October 2018, pp. 1272–1279, 2019, https://doi.org/10.1016/j.wear.2018.12.029.

[15] J. I. Ahuir-Torres, M. A. Arenas, W. Perrie, and J. de Damborenea, "Influence of laser parameters in surface texturing of Ti6Al4V and AA2024-T3 alloys," *Opt. Lasers Eng.*, vol. 103, no. December 2017, pp. 100–109, Apr. 2018, https://doi.org/10.1016/j.optlaseng.2017.12.004.

[16] D. Kümmel, M. Hamann-Schroer, H. Hetzner, and J. Schneider, "Tribological behavior of nanosecond-laser surface textured Ti6Al4V," *Wear*, vol. 422–423, no. January, pp. 261–268, Mar. 2019, https://doi.org/10.1016/j.wear.2019.01.079.

[17] J. Bonse, S. Kirner, M. Griepentrog, D. Spaltmann, and J. Krüger, "Femtosecond Laser Texturing of Surfaces for Tribological Applications," *Materials (Basel).*, vol. 11, no. 5, p. 801, May 2018, https://doi.org/10.3390/ma11050801.

[18] J. Bonse, J. Krüger, S. Höhm, and A. Rosenfeld. "Femtosecond laser-induced periodic surface structures". *J. Laser Appl.* 24, 042006 (2012); https://doi.org/10.2351/1.4712658

[19] F. H. Rajab, C. M. Liauw, P. S. Benson, L. Li, and K. A. Whitehead, "Production of hybrid macro/micro/nano surface structures on Ti6Al4V surfaces by picosecond laser surface texturing and their antifouling characteristics," *Colloids Surfaces B Biointerfaces*, vol. 160, pp. 688–696, Dec. 2017, https://doi.org/10.1016/j.colsurfb.2017.10.008.

[20] B. Li, H. Li, L. Huang, N. Ren, and X. Kong, "Femtosecond pulsed laser textured titanium surfaces with stable superhydrophilicity and superhydrophobicity," *Appl. Surf. Sci.*, vol. 389, pp. 585–593, Dec. 2016, https://doi.org/10.1016/j.apsusc.2016.07.137.

[21] M. Sadeghi, M. Kharaziha, and H. R. Salimijazi, "Double layer graphene oxide-PVP coatings on the textured Ti6Al4V for improvement of frictional and biological behavior," *Surf. Coatings Technol.*, vol. 374, no. June, pp. 656–665, Sep. 2019, https://doi.org/10.1016/j.surfcoat.2019.06.048.

[22] A. Singh, D. S. Patel, J. Ramkumar, and K. Balani, "Single step laser surface texturing for enhancing contact angle and tribological properties," *Int. J. Adv. Manuf. Technol.*, vol. 100, no. 5–8, pp. 1253–1267, Feb. 2019, https://doi.org/10.1007/s00170-018-1579-8.

[23] A. Cunha, A. P. Serro, V. Oliveira, A. Almeida, R. Vilar, and M.-C. Durrieu, "Wetting behaviour of femtosecond laser textured Ti–6Al–4V surfaces," *Appl. Surf. Sci.*, vol. 265, pp. 688–696, Jan. 2013, https://doi.org/10.1016/j.apsusc.2012.11.085.

[24] J. T. Cardoso *et al.*, "Influence of ambient conditions on the evolution of wettability properties of an IR-, ns-laser textured aluminium alloy," *RSC Adv.*, vol. 7, no. 63, pp. 39617–39627, 2017, https://doi.org/10.1039/C7RA07421B.

[25] A.-M. Kietzig, S. G. Hatzikiriakos, and P. Englezos, "Patterned Superhydrophobic Metallic Surfaces," *Langmuir*, vol. 25, no. 8, pp. 4821–4827, Apr. 2009, https://doi.org/10.1021/la8037582.

Submitted: 09.7.2021

Accepted: 22.10.2021

Suzana Jakovljević*
Dražen Mezdić
Gorana Baršić
Faculty of Mechanical Engineering and Naval Architecture, University of Zagreb, Zagreb, Croatia
Hrvoje Skenderović
Institute of Physics, University of Zagreb, Zagreb, Croatia
*Corresponding author:
Suzana.Jakovljevic@fsb.hr